



BELLE2-NOTE-PH-2017-005  
DRAFT Version 1.5  
August 11, 2017

## Analysis Prospects for $B \rightarrow K\pi\pi^0$ with Early Belle II Data

R. Chamberlain\* and M. Barrett†

*Wayne State University, Detroit, MI, USA*

### Abstract

The Belle II detector will become operational in 2018, but using Monte Carlo data, analyses can begin work before then. This analysis aims to create a method that can remove background from  $B^0 \rightarrow K^+ \pi^- \pi^0$  signal events through the use of TMVA, and the quality of the method is preliminarily evaluated with Laura++ software. With more development, this method will be used in CP analyses for the  $B^0 \rightarrow K^+ \pi^- \pi^0$  decay mode.

---

\*Electronic address: rchamber@fandm.edu

†Electronic address: matthew.barrett2@wayne.edu

## Contents

<b>Version History</b>	2
<b>1. Introduction</b>	3
1.1. Purpose and Goals	4
1.2. Simulated Data	4
1.3. Tools	4
1.4. A Note on Further Work	5
<b>2. Event Selection</b>	5
2.1. Initial Cuts	6
2.1.1. Cut Flow Tables I	6
2.2. Continuum Suppression	8
2.2.1. Cut Flow Tables II	8
2.3. Dalitz Plots	9
2.4. Multivariate Analysis (MVA)	11
2.4.1. Decision Trees (BDT)	12
<b>3. Laura++</b>	15
<b>4. Conclusions</b>	16
<b>5. Previous Analysis</b>	16
<b>References</b>	18

## Version History

Version History of this note:

- Version 0.0: Initial version of this document for uploading to Invenio and obtaining a document number. Some text and placeholder plots included.
- Version 1.0: Adding some preliminary tables and figures to the document.
- Version 1.1: Adding the initial sections for a general outline.
- Version 1.2: Starting to fill in some body text and such.
- Version 1.3: Adding in more sections, figures, and filling in text.
- Version 1.4: Further text and figure additions. Implementation of Dr. Barrett's first set of comments.
- Version 1.5: Version to be submitted at end of project.

## 1. INTRODUCTION

Through the use of Monte Carlo simulation data, analyses can be started before the Belle II detector begins taking data, which will expedite many projects. This analysis will study the prospects for data selection in the mode  $B^0 \rightarrow K^+ \pi^- \pi^0$  with the first  $\text{ab}^{-1}$  of data from Belle II. The scope of this project is to create a method that eliminates background for the  $B^0 \rightarrow K^+ \pi^- \pi^0$  decay mode while maintaining enough signal events to analyze the data and search for evidence of CP violation. Although a full CP analysis is the long-term goal of studying this mode, such an analysis was beyond the scope of this project.

A Dalitz plot is a method for visualizing and studying three body decays. In a three body decay, there can be short-lived intermediate particles, called resonances, such as in the case of  $B^0 \rightarrow K^+ \pi^- \pi^0$  where there can be an intermediate  $K^*$  or  $\rho$ . For example,  $B^0 \rightarrow K^{*+} \pi^-$ , and  $K^{*+} \rightarrow K^+ \pi^0$ . These resonances will show up in the Dalitz plots as bands in the plot corresponding to the mass of the resonance. Figure 1 demonstrates this with each resonance band having its own color.

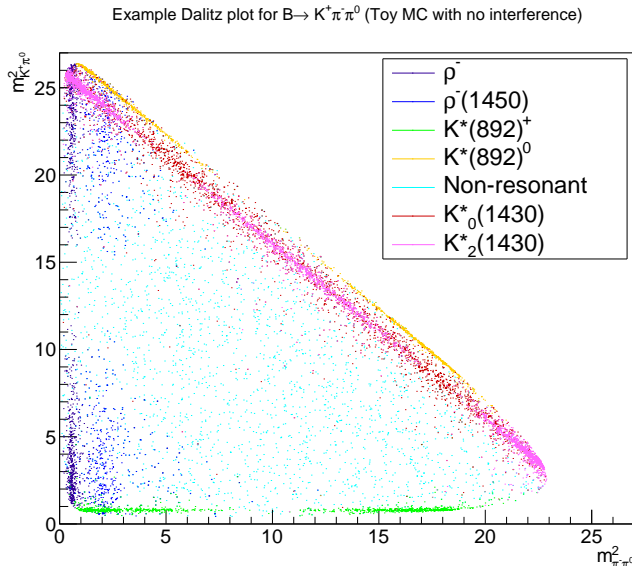


FIG. 1: A plot showing different resonance bands in multiple colors made from simulated data. This is not reflective of actual data, which would not have colors to differentiate the resonances.

Charge-Parity (CP) violation is the property of particles to have different behavior between a particle and its anti-particle. There are three main types of CP violation: direct CPV, CPV in mixing, and CPV in interference. Study of this mode will focus on direct CP violation, which is the difference in the probability of certain decay modes of a particle and its anti-particle; for example, a particular kaon decay mode might happen slightly more often than the decay “anti-mode.” It is possible to not have any CP violation in the inclusive decay mode but to have it in one or more resonant modes.

By studying  $B^0 \rightarrow K^+ \pi^- \pi^0$  via a Dalitz plot method, it will be possible to search for direct CP violation in not just the three body decay, but also the intermediate resonant modes.

### 1.1. Purpose and Goals

This project aims to provide a preliminary method of data selection which is efficient at keeping signal and significantly reduces background events. Other previous analyses of  $K\pi\pi$  decay modes, in which all three particles are charged, have observed several thousand events after cuts. The decay mode of this analysis has a neutral pion, which makes accurate reconstruction more difficult to achieve. Nonetheless, this project aims to have roughly one to two thousand signal events after data selection processes. However, since there are always inadequately reconstructed signal events and a chance that the copious background can mimic signal properties, there will inevitably be signal events that are lost and background events that are not. Therefore, maximizing the background rejection and signal efficiency is the primary measure of success for this aspect of the analysis. An example of a background rejection vs. signal efficiency plot is shown in figure 2.

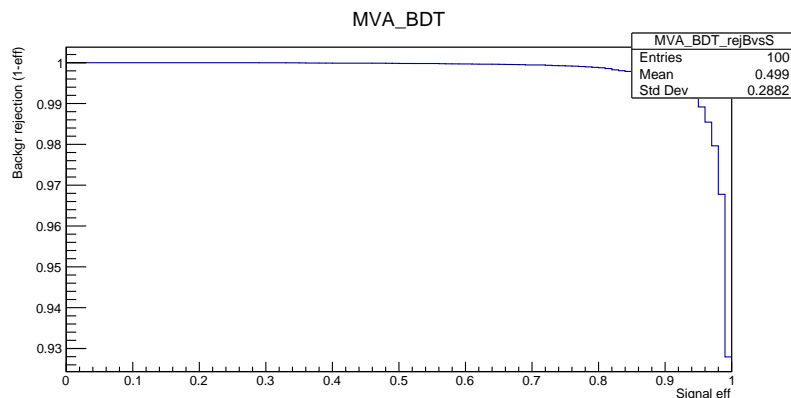


FIG. 2: An example ROC curve for the BDT MVA method (discussed in more detail in 2.2.4.2.4.1).

### 1.2. Simulated Data

MC8 is the eighth set of Monte Carlo simulated data that Belle II has produced for use in analysis. For this analysis, MC8 campaign data samples were used. The signal sample was, of course, for  $B^0 \rightarrow K^+ \pi^- \pi^0$ , and the background samples used were from  $u\bar{u}$ , mixed, and charged blocks.  $u\bar{u}$  sample was chosen as a representative for the continuum background data, but other continuum samples should be tested. Summarized from the MC8 Phase III table on DESY's Confluence, table I shows the sample type, number of events per  $1 \text{ ab}^{-1}$  of data, and the location of a few datasets on KEKCC [1].

### 1.3. Tools

To develop the analysis for this project and evaluate it, two tools were used significantly: Laura++ [3] for fitting and fit analysis, and TMVA [4] for creating multivariate analyses (MVA) and picking the best-performing MVA. In addition to these, `basf2` [5] and the Belle II grid were heavily used for reconstruction of MC8 data samples.

TABLE I: A table which provides some basic information from the MC8 generic samples page. \*Signal sample information is from the signal samples page [2]. It is not proportional to  $1 \text{ ab}^{-1}$  of data and it is not included in the total.

Sample type	Number of events $\times 10^6$	LPN
$u\bar{u}$	1605	prod00000966/s00/e0000/4S/r00000/uubar
mixed	534.6	prod00000962/s00/e0000/4S/r00000/mixed
charged	565.4	prod00000964/s00/e0000/4S/r00000/charged
$d\bar{d}$	401	prod00000968/s00/e0000/4S/r00000/ddbar
$s\bar{s}$	383	prod00000970/s00/e0000/4S/r00000/ssbar
$c\bar{c}$	1329	prod00000972/s00/e0000/4S/r00000/ccbar
<b>total</b>	<b>4818</b>	
signal*	2.0	prod00001967/s00/e0000/4S/r00000/1110022000/sub00

#### 1.4. A Note on Further Work

This project was a ten-week summer program; as such, many aspects of a full analysis were missed. Several tasks should be done or improved to make this analysis more robust which there was not enough time to do initially. A basic yet important part of an analysis such as this would be to separate the decay into  $B^0$  and  $\bar{B}^0$ . This is essential for examining the CP violation of this mode, which would also require looking at B meson vertex information. This will be pursued in the future. Another possible addition to this analysis would be to test more multivariate analysis techniques. Additionally, as stated in section 1.1.2, testing more background samples, especially from the continuum, would improve the quality of this analysis. An error analysis has not been looked at either; the only errors which have been examined are those returned from Laura++ fitting. Of the full MC8 signal data sample, 74.37% of events had only one candidate, exemplified in figure 3, so best candidate selection was not studied in detail during this project, and events with more than one candidate were picked pseudo-randomly from the possibilities. Finally, variables such as  $\Delta E$  and  $M_{BC}$  were included in the multivariate analysis since this was an optimal way to optimize the signal to background ratio on a short timescale. With more time to improve the selection, these variables would be considered separately to allow for study of, for example, background sidebands.

## 2. EVENT SELECTION

To winnow down the data, there is a set of multiple steps to figure out the best cuts to make. First, there was an initial processing of MC8 data samples which also performed a reconstruction of the data. The reconstruction took all the  $K$ ,  $\pi$ , and  $\pi^0$  candidates and made all possible combinations; ultimately, it would return the combinations which pass initial loose selection cuts. After that, basic cuts were applied to the data in order to see how they would affect the data and number of events still viable (see 2.2.1). Following the basic cuts, continuum suppression variables were brought in to eliminate the continuum background more effectively (discussed in 2.2.2). In the last step of this project, a multivariate analysis (MVA) was used to more efficiently keep the signal while getting rid of the continuum

background (described in 2.2.4).

## 2.1. Initial Cuts

The first step of data selection was to make general cuts to the events. This reduction of events used many individual variables on which to place limits. The variables used and the limits set on them are listed below, and the effects of these cuts are shown in tables II and III and are discussed in section 2.2.1.2.1.1.

- 0, No cuts: the total number of events that would be started with.
- 1, Initial processing with a reconstruction steering file: Cuts applied here: `massVertexRave` at a value of 0.15 (15% confidence rate),  $5.24 < M_{BC} < 5.29$ , and  $|\Delta E| < 1.0$ .  
ROE masks:  $nCDCHits > 0$ ,  $useCMSFrame(p) \leq 3.2$ ,  $p \geq 0.05$
- 2,  $M_{BC}$ :  $5.27 < M_{BC} < 5.29$
- 3,  $\Delta E$ :  $|\Delta E| < 0.02$
- 4, mass of the  $\pi^0$ :  $0.120 < m_{\pi^0} < 0.148$
- 5, error of mass for  $\pi^0$ :  $Err(m_{\pi^0}) < 0.01$
- 6, number of candidates per event:  $nCands < 100$

These cuts were chosen because of their ability to distinguish background and low-quality signal events from higher-quality signal events. For example, background data will have a higher error on the mass of the  $\pi^0$  than good signal data. The variable `nCands` tells how many reconstructed candidates a particular event has, so the fewer the possible candidates, the more likely that the selected reconstruction is correct, thus there is a very loose limit on the variable `nCands`.  $M_{BC}$  is the beam energy constrained mass, and  $\Delta E$  is the difference between the energy of the reconstructed B meson and the energy of the beam [6]. Placing constraints on these two variables is an established practice for differentiating signal and background events.

### 2.1.1. Cut Flow Tables I

Tables II and III are cut flow tables used to help determine the effectiveness of some basic cuts to the data, listed above. In the cut flow tables of this note, the column “Bkg Evt” is the sum of the events from background samples  $u\bar{u}$ , charged, and mixed. Table II shows the effects of cuts to the unscaled number of events; the numbers shown come directly from processing the data files of MC8, which means that the proportion of signal to background events is not what would be expected from real data. During collisions, the ratio of  $B^0 \rightarrow K^+ \pi^- \pi^0$  signal to background events would be significantly smaller. Table III presents the number of events scaled to roughly how many events would be in  $1 \text{ ab}^{-1}$  of data.

To calculate the scaling factors for the signal, the following values are needed: the number of  $B^0$  events in a collision (taken to be roughly 534.6 million from the mixed background

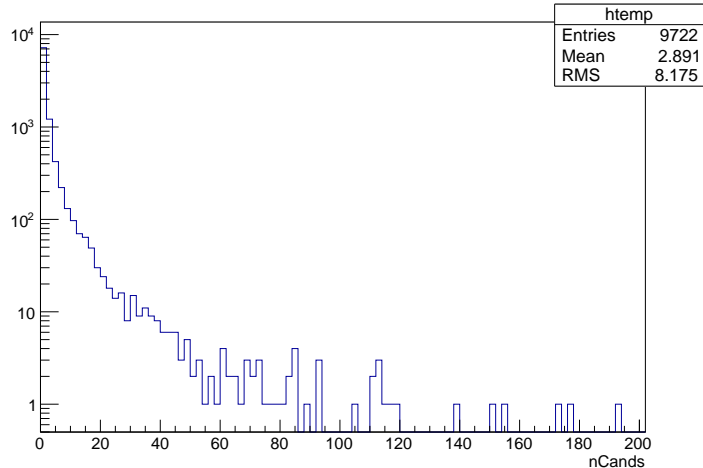


FIG. 3: A histogram showing the variable nCands for one signal file after initial processing and reconstruction. For ability to see bins with few events, the y-axis is on a log scale.

sample) and the branching fraction of the  $B^0 \rightarrow K^+ \pi^- \pi^0$  mode, which is  $3.78 \times 10^{-5}$  [7]. Equation 1 presents this calculation.

$$\begin{aligned}
 scale_{signal} &= (\text{number of } B^0 \text{ events}) \times (\text{branching fraction}) / (\text{number of events in dataset}) \\
 &= (5.346 \times 10^8) \times (3.78 \times 10^{-5}) / (2 \times 10^6) = 0.010104
 \end{aligned} \tag{1}$$

It should be noted that this analysis did not use the full background datasets due to processing time and time to download the processed files from the grid; instead, a partial sub-block of the three data samples ( $u\bar{u}$ , mixed, and charged) were used in the data processing. Thus, scaling up the number of events was necessary. To calculate the scaled number of background events, the number of background events in  $1 \text{ ab}^{-1}$  and the number of events used in the analysis are needed. This calculation is shown in equation 2. For each background sample, the numbers are different, so the calculation is only general.

$$scale_{background} = (\text{number of events in full dataset}) / (\text{number of events used in analysis}) \tag{2}$$

As can be seen in table III in particular, the separate cuts on variables for  $M_{BC}$  and  $\Delta E$  do not change much with respect to the number of events because the figure of merit (FoM) does not change significantly between the cuts. Even though the variables' effects on the data are similar, they are both kept in the analysis for their physical significance, such as for defining signal regions and side bands.

The figure of merit is calculated as described in equation 3:

$$\begin{aligned}
 FoM &= (\text{number of signal events}) / \sqrt{(\text{number of signal events}) + (\text{number of background events})} \\
 &= \frac{S}{\sqrt{S + B}}
 \end{aligned} \tag{3}$$

TABLE II: A table showing the effects of basic cuts on the raw, unscaled number of events.

Cut	Signal Evt	Signal Eff	Bkg Evt	Bkg Eff	$u\bar{u}$ Evt	Charged Evt	Mixed Evt
none	$2 \times 10^6$	100	$1.155 \times 10^8$	100	$3.15 \times 10^7$	$5.25 \times 10^7$	$3.15 \times 10^7$
init	98139	4.90695	54509	0.0471939	52274	1344	891
$M_{BC}$	88088	4.4044	15954	0.013813	15181	321	452
$\Delta E$	88052	4.4026	15755	0.0136407	15005	307	443
$m_{\pi^0}$	75131	3.75655	8533	0.00738788	8109	175	249
$\text{Err}(m_{\pi^0})$	71150	3.5575	6275	0.0054329	5948	136	191
nCands	71106	3.5553	6230	0.00539394	5903	136	191

TABLE III: A table showing the effects of basic cuts on number of events scaled to  $1 \text{ ab}^{-1}$  of data.

Cut	Signal Evt	Signal Eff	Bkg Evt	Bkg Eff	$u\bar{u}$ Evt	Charged Evt	Mixed Evt	FoM
none	20207.9	100	$2.705 \times 10^9$	100	$1.605 \times 10^9$	$5.654 \times 10^8$	$5.346 \times 10^8$	0.38854
init	991.591	4.90695	$2.6931 \times 10^6$	0.0995594	$2.663 \times 10^6$	14474.2	15121.5	0.604126
$M_{BC}$	890.036	4.4044	784636	0.0290069	773508	3457.02	7671.09	1.00422
$\Delta E$	889.672	4.4026	775365	0.0286641	764540	3306.24	7518.34	1.00978
$m_{\pi^0}$	759.119	3.75655	419283	0.0155003	413173	1884.67	4225.89	1.17129
$\text{Err}(m_{\pi^0})$	718.895	3.5575	307771	0.0113779	303065	1464.66	3241.54	1.29433
nCands	718.451	3.5553	305478	0.0112931	300772	1464.66	3241.54	1.29837

## 2.2. Continuum Suppression

The continuum ( $e^+e^- \rightarrow q\bar{q}$ ;  $q$  is  $u$ ,  $d$ ,  $s$ , or  $c$ ) is a type of event distinct from  $B\bar{B}$  decay events.  $B\bar{B}$  decays have spherical shapes due to the low velocity of the mesons in the center of mass frame, whereas continuum events have event shapes that are jet-like because they are not at rest on the center of mass frame; daughters are boosted in a particular direction [6]. Since continuum events are produced three times more than those from  $B\bar{B}$  [8], it is imperative to get rid of as many continuum events as possible while maintaining signal efficiency. There exist many variables to separate  $B\bar{B}$  events from the continuum; event shape elements and thrust quantities were found to be most useful in this part of the analysis.

### 2.2.1. Cut Flow Tables II

For the continuum, the variables which were included for cuts were:

- 1, ThrustB:  $\text{Thrust}B < 0.95$
- 2,  $h^{so}(0,4)$ :  $hso04 < 0.4$
- 3,  $h^{so}(1,2)$ :  $hso12 < 0.4$



The effects of these cuts are shown in tables IV and V.

Figures 4, 5, and 6 show the distributions of these variables for signal and background; the left image of each shows the signal and background curves scaled to have the same area, and the right image shows the curves unscaled. The scaled images are to compare the relative shapes of the distributions, and the unscaled images are to show the proportions of the data.

TABLE IV: A table showing the effects of continuum suppression cuts on the raw, unscaled number of events.

Cut	Signal Evt	Signal Eff	Bkg Evt	Bkg Eff	$u\bar{u}$ Evt	Charged Evt	Mixed Evt
prev	71106	3.5553	6230	0.00539394	5903	136	191
ThrustB	50422	2.5211	1116	0.000966234	962	68	86
$h^{so}(0,4)$	50150	2.5075	1049	0.000908225	901	66	82
$h^{so}(1,2)$	50104	2.5052	1007	0.000871861	859	66	82

TABLE V: A table showing the effects of continuum suppression cuts on number of events scaled to 1  $\text{ab}^{-1}$  of data.

Cut	Signal Evt	Signal Eff	Bkg Evt	Bkg Eff	$u\bar{u}$ Evt	Charged Evt	Mixed Evt	FoM
prev	718.451	3.5553	305478	0.0112931	300772	1464.66	3241.54	1.29837
ThrustB	509.461	2.5211	51208.1	0.00189309	49016.2	732.328	1459.54	2.24023
$h^{so}(0,4)$	506.713	2.5075	48010.5	0.00177488	45908.1	710.789	1391.66	2.30045
$h^{so}(1,2)$	506.248	2.5052	45870.5	0.00169577	43768.1	710.789	1391.66	2.35078

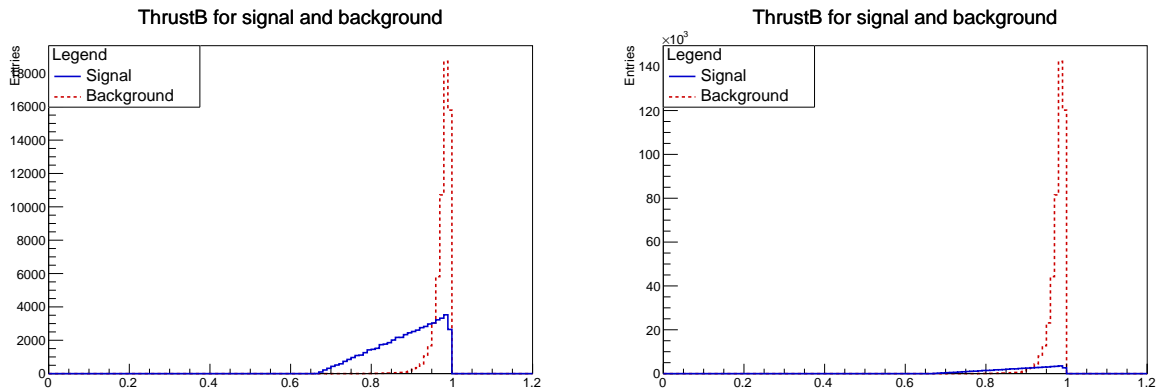


FIG. 4: ThrustB distribution for signal and background; scaled left, unscaled right.

### 2.3. Dalitz Plots

Another aspect of an analysis like this is the efficiency of the cuts being consistent over a Dalitz plot. A Dalitz plot is used to show the kinematics of a three-body decay using the

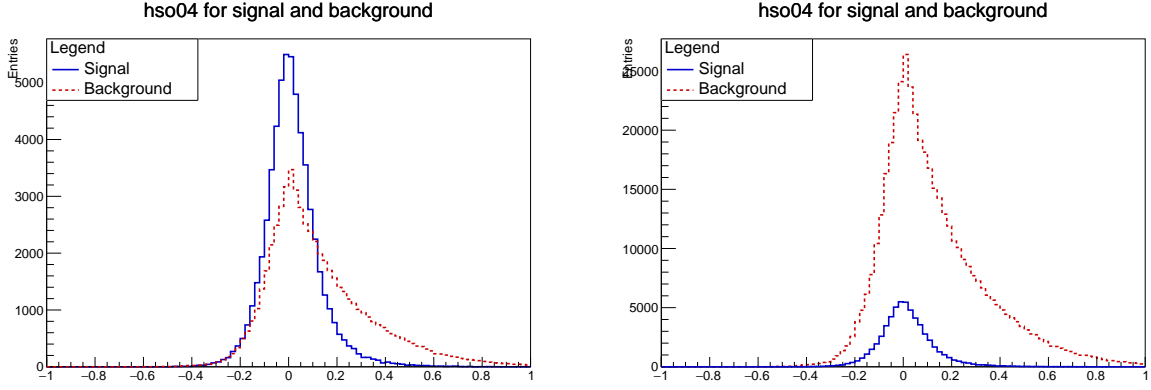


FIG. 5:  $h^{so}(0,4)$  distribution for signal and background; scaled left, unscaled right.

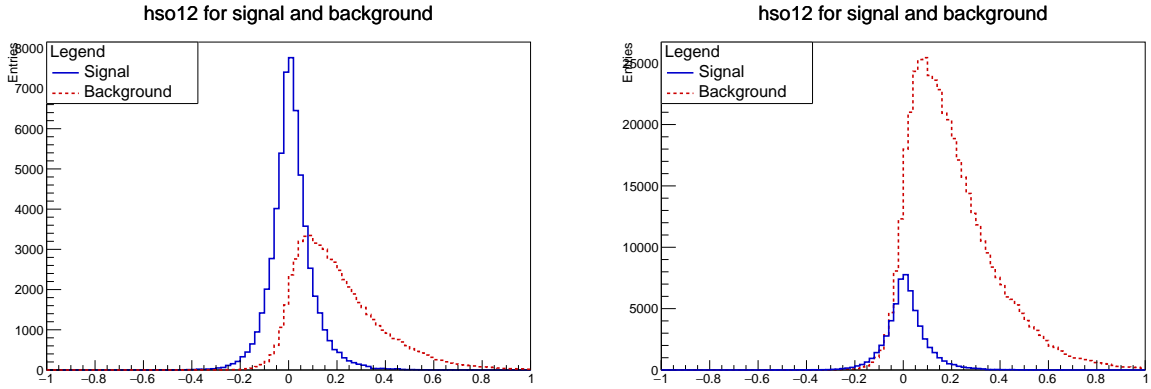


FIG. 6:  $h^{so}(1,2)$  distribution for signal and background; scaled left, unscaled right.

squared mass of two combinations of the three daughters. If there are any resonances in the decay, they will show up as lines on the plot, and their positions (vertical, horizontal, or diagonal) indicate which two particles came from the resonant particle.

In addition to seeing signatures of resonances, Dalitz plots are useful for seeing how data is affected during the analysis and event selection processes. Shown in figure 7 are Dalitz plots which display the efficiency of the basic cuts on the signal (left) and on the self crossfeed (right) events over the plot. This is done by dividing the Dalitz plot after cuts by one that has the truth data, the latter being created by a module (created by Dr. Matthew Barrett) with basf2. As is expected, the efficiency of the cuts is significantly lower around the kinematic boundaries where there are very low-momentum particles that are easily misreconstructed. The particles most likely to be misreconstructed are  $\pi^0$  mesons. This is because  $\pi^0$  decays into two photons; during reconstruction of the event, there can be many photon candidates from other particles or calorimeter noise, which can produce many fake  $\pi^0$ . As such, the self crossfeed plot has a higher efficiency in the corner representing the low momentum  $\pi^0$ .

Also provided in figure 8 are the Dalitz plots for the two kinds of background used in this project:  $u\bar{u}$  (left) and  $B\bar{B}$  (right). These are unscaled plots (not proportional to  $1 \text{ ab}^{-1}$

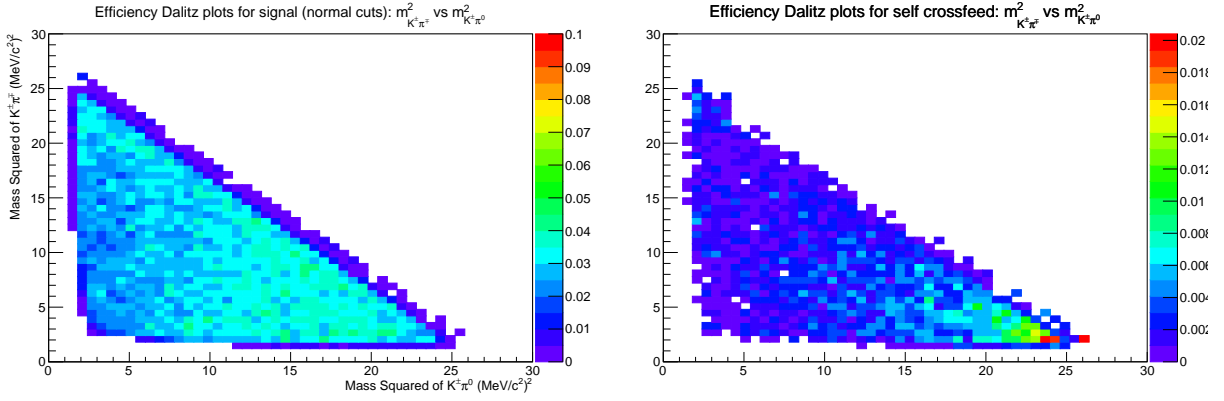


FIG. 7: Efficiency Dalitz plot using the Dalitz Truth module output with simple cuts on the signal events (left) and self crossfeed events (right). Note that the color scales are not the same for both plots.

of data) without any cuts made aside from those applied during the initial processing and reconstruction.

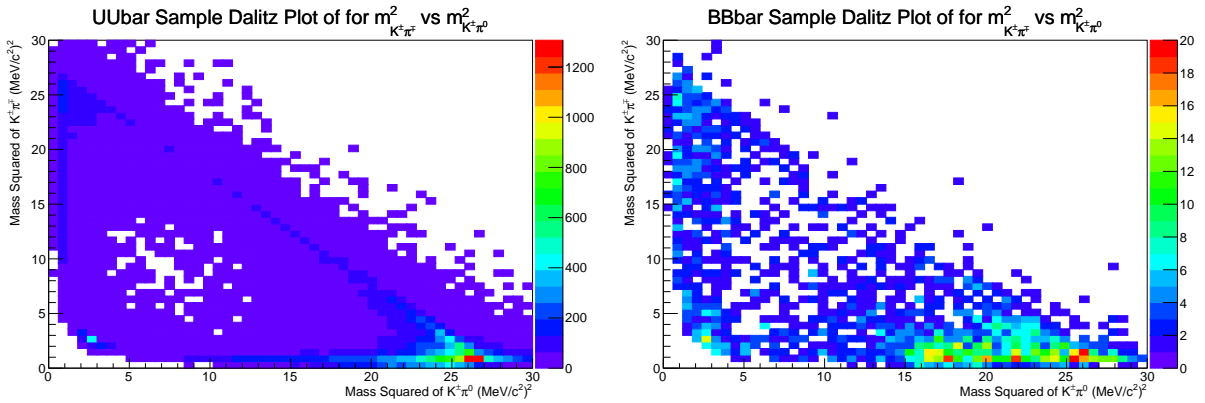


FIG. 8: Dalitz plots for the background samples  $u\bar{u}$  (left) and mixed + charged (right). Plots are for unscaled number of events without any cuts aside from initial processing.

## 2.4. Multivariate Analysis (MVA)

Multivariate analyses (MVA) are methods of data selection which take multiple variables into account simultaneously. This method differs from a series of cuts because each cut only considers one variable at a time when determining whether to keep events or not. Oftentimes multivariate analyses mimic human selection processes and are much more efficient at keeping signal events and rejecting background. There are many different statistical models to choose from when doing an MVA.

ROOT [9] has a built-in MVA program called TMVA that uses training and testing data to come up with methods of data selection. This program was used to test several MVA

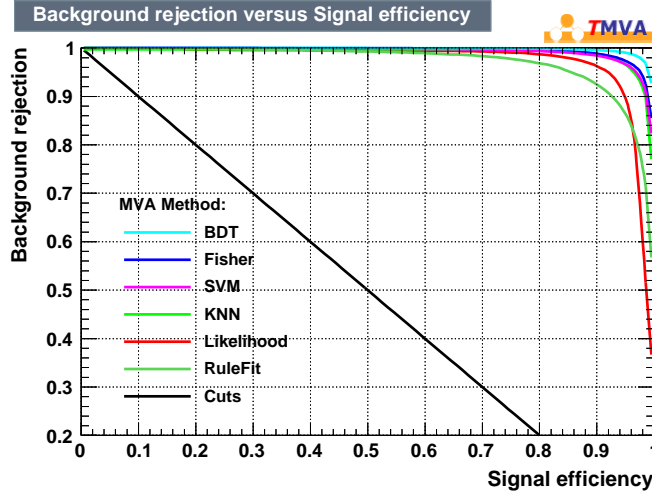


FIG. 9: An ROC curve made automatically by TMVA [4] showing background rejection vs. signal efficiency for several MVA methods.

methods on the data and judge which method would best suit this analysis. Only the method which proved best to this project is discussed (section 2.2.4.2.4.1). Additionally, figure 9 is a background rejection vs. signal efficiency plot of the multiple MVA models which TMVA applied to the data. The best MVA method is the one for which the background rejection and signal efficiency are maximized.

#### 2.4.1. Decision Trees (BDT)

A decision tree (DT) is a method of multivariate analysis that poses a set of questions, each of which only has two possible answers, dependent on the answers to the previous questions in order to determine if an event is signal or background [10]. Most often, several DTs are used in a single examination of the dataset in order to get the best result. For this analysis, the BDT method performed best on the data throughout the multiple iterations of improving the MVA. Figure 9 shows in a cyan line that the BDT method was closest to 100% background rejection and 100% signal efficiency.

When the analysis is created for the BDT method, a BDT variable is created, and cuts can be made to the data on this variable. The histograms in figure 10 show the distribution of the BDT variable for the signal and  $u\bar{u}$  samples. On the histogram, there is a green vertical line at 0.3; the cut on BDT to this data was  $BDT > 0.3$ . Figure 11 shows the efficiencies of 1000 signal (blue) events and 1000 background (red) events depending on the cut made on BDT variable. In green is a curve representing the figure of merit (as described in 3). The peak of the figure of merit curve changes value depending on the number of background and signal events.

Only 4.1% of the signal events remain from the unprocessed dataset after the BDT cut; however, of the signal events remaining from the initial processing and reconstruction and a cut on  $nCands$ , 85% was retained after the cut to the BDT variable. This is shown in the “Signal Evts” column of tables VI and VII. In the “Bkg Evts” column of table VII (data scaled to  $1 \text{ ab}^{-1}$ ), only  $5.8 \times 10^{-4}$  % of the events remain after the cut on BDT. This amounts

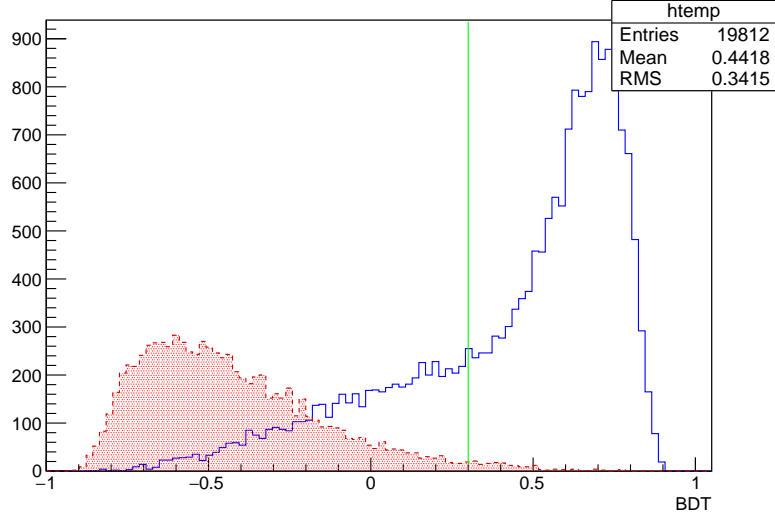


FIG. 10: Histogram showing the generated BDT variable for signal (blue, unfilled) and  $u\bar{u}$  (red, filled) samples. A green vertical line marks the cut on BDT ( $\text{BDT} > 0.3$ ).

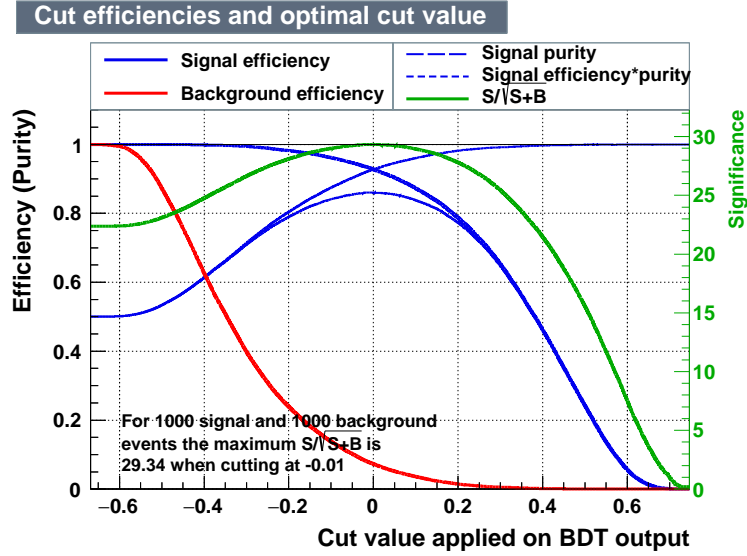


FIG. 11: A curve made automatically by TMVA [4] showing the efficiency curves of signal and background events from the BDT model. A curve showing the figure of merit ( $S/\sqrt{S+B}$ ) is also plotted in green.

to a roughly 1:2 ratio of signal to background (scaled event numbers) after processing, and thus this would be what to expect using an analysis like this on  $1 \text{ ab}^{-1}$  of data.

Figure 12 shows the efficiency Dalitz plot using the BDT cut instead of the basic cuts. As compared to the signal efficiency plot in figure 7 (left), figure 12 has overall better efficiency. Also, it can be noted that the background Dalitz plots after the BDT cut (figure 13) are significantly more empty than in 8. Both are unscaled, so in  $1 \text{ ab}^{-1}$  of data, there

would be more entries in more bins.

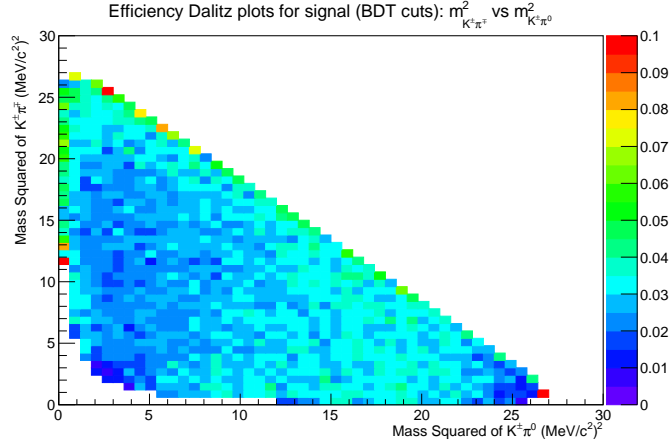


FIG. 12: Efficiency Dalitz plot for signal events using the BDT cut and the Dalitz Truth module output.

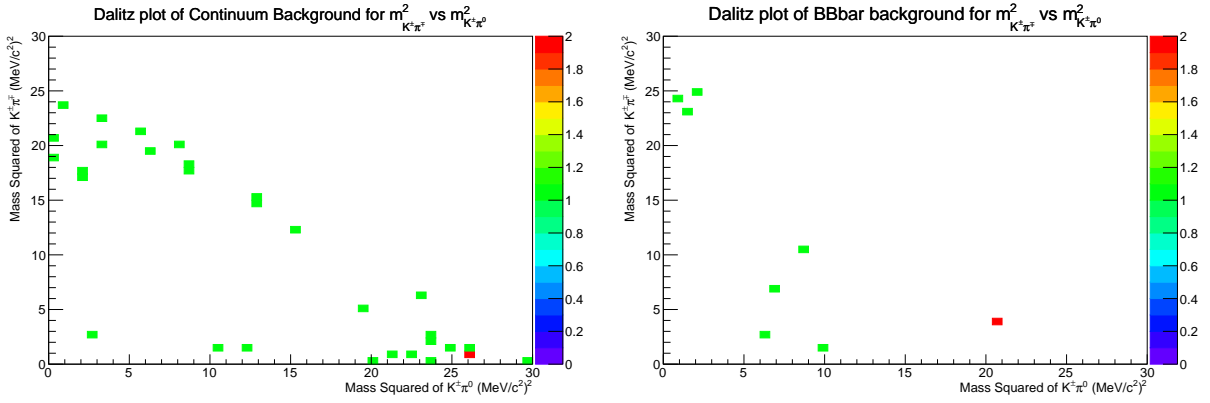


FIG. 13: Dalitz plots for the background samples  $u\bar{u}$  (left) and mixed + charged (right). Plots are for unscaled number of events after BDT cut.

The variables included in this MVA are the following:

- ThrustB, the magnitude of B thrust axis [11]
- ThrustO, the magnitude of the ROE thrust axis
- CosTBTO, the cosine of the angle between the thrust axes of the B and the ROE
- CosTBz, the cosine of the angle between the B thrust axis and the z-axis
- R2, the reduced Fox-Wolfram moment  $R_2$
- mm2, the square of the missing mass

- $E_T$ , transverse energy
- $h^{so}$  and  $h^{oo}$  variables, the normalized Fox-Wolfram moments
- $M_{BC}$
- $\Delta E$
- $m_{\pi^0}$
- $\text{Err}(m_{\pi^0})$

In a longer analysis,  $\Delta E$  and  $M_{BC}$  would have been left out of the MVA in order to examine them in other contexts, such as background sidebands, as mentioned in 1.1.4. However, the short timespan did not allow for such analyses and including  $\Delta E$  and  $M_{BC}$  proved effective in the MVA.

TABLE VI: Using the previous cuts *in* the MVA instead of *before* the MVA. Unscaled data.

Cut	Signal Evts	Signal Eff	Bkg Evts	Bkg Eff	$u\bar{u}$ Evts	Charged Evts	Mixed Evts
none	$2 \times 10^6$	100	$1.155 \times 10^8$	100	$3.15 \times 10^7$	$5.25 \times 10^7$	$3.15 \times 10^7$
init	98139	4.90695	59551	0.0515593	57316	1344	891
nCands	97955	4.89775	59154	0.0512156	56935	1335	884
BDT	83735	4.18675	40	$3.4632 \times 10^{-5}$	31	2	7

TABLE VII: Using the previous cuts *in* the MVA instead of *before* the MVA. Scaled to  $1 \text{ ab}^{-1}$ .

Cut	Signal Evts	Signal Eff	Bkg Evts	Bkg Eff	$u\bar{u}$ Evts	Charged Evts	Mixed Evts	FoM
none	20207.9	100	$2.705 \times 10^9$	100	$1.605 \times 10^9$	$5.654 \times 10^8$	$5.346 \times 10^8$	0.38854
init	991.591	4.90695	$2.9499 \times 10^6$	0.109057	$2.920 \times 10^6$	14474.2	15121.5	0.57723
nCands	989.731	4.89775	$2.9303 \times 10^6$	0.108331	$2.901 \times 10^6$	14377.3	15002.7	0.57807
BDT	846.053	4.18675	1719.86	$6.3581 \times 10^{-5}$	1579.52	21.539	118.8	16.7023

### 3. LAURA++

Laura++ [3] is a tool used for simulated (MC) data generation and fitting of the data, MC or experimental. The program uses a maximum likelihood fit to a multidimensional function which includes functions to describe lineshapes of different resonance components. It was used near the beginning of this project for generation of Toy Monte Carlo data and initial fitting of raw data, and again at the end it was used for fitting data to which the MVA cut was applied.

Included in the final fits were three resonances, a signal efficiency Dalitz plot, and a Dalitz plot for each the  $u\bar{u}$  and the  $B\bar{B}$  (mixed + charged) background samples. Providing these files to Laura++ allows the program to better fit the data since it has more information. However, since the cut on the BDT variable left so little background in the unscaled data

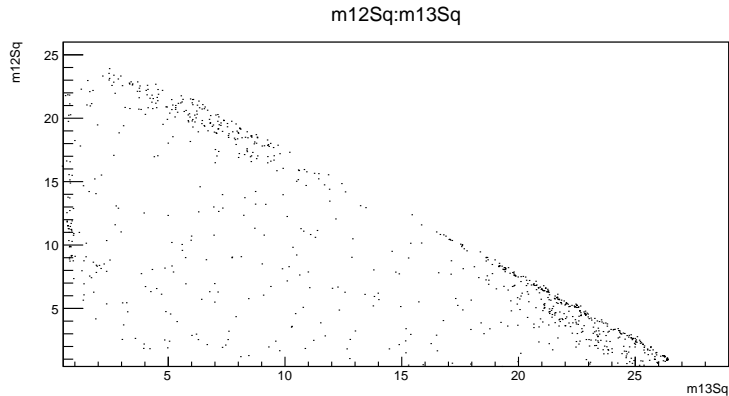


FIG. 14: A Dalitz plot of the data generated by Laura++. The background included in this in the input options in unscaled after reduction from the cut of BDT.

(see figure 13), each bin with data made a stark contrast against an empty bin, making the background Dalitz plots very difficult to fit. As such, Laura++ did not always successfully complete the fits to the data. However, with only nine  $B\bar{B}$  events and thirty-one  $u\bar{u}$  events provided for fitting, the amplitudes of the resonances were determined reasonably well.

#### 4. CONCLUSIONS

Ultimately, for this project, a significant measure of success is the pull plot created by the Laura++ fitting. A pull plot should have a mean of zero and a width of one, and it tells how closely the fit matches the actual data. When generating data in Laura++, the program will create many sets of data from the same input parameters, called experiments, the number of which can be adjusted. When fitting, it is best to fit the same experiment many times due to multiple solutions from secondary minima. Typically, pull plots from Laura++ are made from many fits, on the order of hundreds, of a hundred experiments. However, fitting the data is a time-consuming process, so it was not practical to do this in the time of this project. The pull plot in figure 15 is therefore sparsely populated with the successful fits of the fifty attempted.

This project as gone through the entire chain of steps that an analysis should, though each step has the possibility to be improved. Many of these improvements and the further work is discussed in section 1.1.4.

#### 5. PREVIOUS ANALYSIS

In 2014, there was a Belle note describing an uncompleted Belle analysis of the  $B^0 \rightarrow K^+ \pi^- \pi^0$  mode using Dalitz plots [8]. This project referenced that note, as this is somewhat of a continuation of the note. The analysis of this paper differs in its scope and goals due to amount of time available to this project. However, a future goal of this analysis is to finish the work started in the aforementioned note.



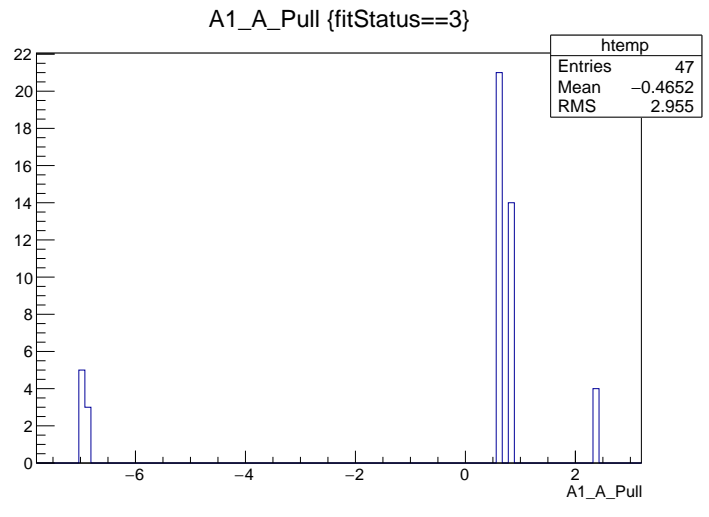


FIG. 15: A pull plot of the fit for the second resonance included in the data generation.

- 
- [1] *Belle II internal wiki: MC8 Phase III -  $Y(4S)$  generic samples*, <https://confluence.desy.de/display/BI/MC8+Phase+III+-+Y%284S%29+generic+samples>.
- [2] *Belle II internal wiki: MC8 Phase III -  $Y(4S)$  signal samples*, <https://confluence.desy.de/display/BI/MC8+Phase+III+-+Y%284S%29+signal+samples>.
- [3] T. Latham, *The Laura++ Dalitz plot fitter*, AIP Conf. Proc. **1735** (2016) 070001, [arXiv:1603.00752](https://arxiv.org/abs/1603.00752) [physics.data-an].
- [4] A. Hoecker, P. Speckmayer, J. Stelzer, J. Therhaag, E. von Toerne, and H. Voss, *TMVA: Toolkit for Multivariate Data Analysis*, PoS **ACAT** (2007) 040, [arXiv:physics/0703039](https://arxiv.org/abs/physics/0703039).
- [5] *Belle II internal wiki: Basf2manual*, <https://confluence.desy.de/display/BI/Software+Basf2manual>.
- [6] A. J. Bevan et al., Belle, BaBar, *The Physics of the B Factories*, Eur. Phys. J. **C74** (2014) 3026, [arXiv:1406.6311](https://arxiv.org/abs/1406.6311) [hep-ex].
- [7] C. Patrignani et al., Particle Data Group, *Review of Particle Physics*, Chin. Phys. **C40** (2016) no. 10, 100001.
- [8] M. Petrič, Belle II, *Measurement of CP Violation in  $B^0 \rightarrow K^+ \pi^- \pi^0$  Using a Dalitz Plot*, .
- [9] R. Brun and F. Rademakers, *ROOT: An object oriented data analysis framework*, Nucl. Instrum. Meth. **A389** (1997) 81–86.
- [10] KIT, C. Boser et al., *Introduction to Boosted Decision Trees*, <https://indico.scc.kit.edu/indico/event/48/session/4/contribution/35/material/slides/0.pdf>. Accessed:2017-08-04.
- [11] *Belle II internal wiki: Physics NtupleTool*, <https://confluence.desy.de/display/BI/Physics+NtupleTool>.